Photovoltaic Properties of Poly (3-Hexylthiophene): [6, 6]-Phenyl C61-Butyric Acid 3-Ethylthiophene Thin Films

B.M. Omer[1,2,*]

[1] Department of Physics, College of Science and Arts-Ranyah, Taif University, Kingdom Saudi Arabia
[2] Department of Applied Physics, Faculty of Applied Science and Computer, Omdurman Ahlia University,
P.O.Box 786, Omdurman-Sudan

We fabricated and studied the electrical and photovoltaic properties of organic solar cell based on poly (3-hexylthiophene) (P3HT) as an electron donor blended with the acceptor [6, 6]-Phenyl C61-Butyric Acid 3-Ethylthiophene Ester (modified fullerene). The active layer composed of (3:1, w/w) mixture of P3HT and the modified fullerene was sandwiched between indium tin oxide (ITO) and aluminum (Al). The ideality factor n and barrier hight φ_b values were determined from the dark current density-voltage characteristics and found as 2.45 and 0.78 eV, respectively. The device shows photovoltaic behavior with an open circuit voltage of 400 mV, short circuit current of 22.9 μA/cm^2 and fill factor 0.32 under 2.8 mW/cm^2 light intensity.

Keywords: Poly3-Hexylthiophene, Modified fullerene, Organic solar cell, Open circuit voltage.

PACS numbers: 78.66.Qn, 78.40.Me

1. INTRODUCTION

Since the discovery of the conjugated polymers, rectifying junctions such as p-n junction and Schottky junctions have been studied as to explore the possible application of conjugated polymers [1-4]. Polymer solar cells have attracted considerable attention due to their low cost, lightweight [5], as well as their potential application in flexible large area devices [6].

Despite the low cost, the power conversion efficiency of bulk hetrojunction devices is low compared to inorganic solar cells. Recently Yong Cao et al reported an efficiency of 9.2 % for a photovoltaic cell with a bulk heterojunction inverted structure [7]. Bulk heterojunction photovoltaic consists of an intimate blend of a conjugated polymer and an electron acceptor that form an interpenetrating network with percolated paths to both electrodes [8]. When light is incident on the device, excitons are created on the polymer chains. If an exciton is able to diffuse within its lifetime to an electron acceptor, it will be quenched with near unit quantum yield, creating a spatially separated electron-hole pair with the hole localized on the polymer chain and the electron on the acceptor molecule. Under the influence of the built-in electric field, these initially bound charges can then separate and migrate to the electrodes, thus producing a photocurrent.

So far, research efforts in solution-processed organic photovoltaic materials have been dominated by the use of one particular fullerene derivative, [6, 6]-Phenyl C61-Butyric acid methyl ester (PCBM), as the electron acceptor. But PCBM is not necessarily the optimum acceptor for solution processed organic photovoltaic materials. The preparation of different derivatives of C60 fullerenes and their use in bulk heterojunction polymer solar cells was reported by different authors [9-11].

To our knowledge there is no published study on the photovoltaic properties of P3HT: [6, 6]-Phenyl C61-Butyric Acid 3-Ethylthiophene Ester (**Modified full-erene**) thin films. In this paper, we report the fabrication and characterization of bulk heterojunction solar cell based on Poly (3-Hexylthiophene) and [6, 6]-Phenyl C61-Butyric Acid 3-Ethylthiophene Ester with (3:1) composite ratio.

2. EXPERIMENTS

The organic photovoltaic cell in this study consists of a layer of poly (3-Hexylthiophene) / [6, 6]-Phenyl C61-Butyric Acid 3-Ethylthiophene Ester blend thin film sandwiched between transparent anode indium tin oxide (ITO) and metal cathode aluminum (Al). The p-type donor polymer P3HT and the n-type acceptor modified fullerene in the active layer were purchased from sigma-Aldrich Corporation and American Dye Source, Inc. respectively; the chemical structures are shown in Fig. 1. All materials were used as received without further purification. Before device fabrication the ITO coated glass substrate was first etched and patterned to serve as anode. The substrate was cleaned with Isopropyl alcohol and acetone in an ultrasonic bath each for 15 min sequentially. To make a P3HT/modified fullerene (3:1, w/w) solution, P3HT (16.26 mg) and modified fullerene (5.48 mg) were dissolved in 1,2 dichlorobenzene (concentration 21.74 mg/ml). The blend was spin coated onto the substrates with atypical spinning speed and time at 2000 rpm for 40 s. Finally Al metal was vacuum-deposited to form the cathode. The active area of the device, defined by shadow mask, was 0.07 cm^2 .The structure of the device is shown in Fig. 2.

For the UV-vis absorption measurements, the solutions were spin coated onto quartz substrates, the properties of the relevant films were obtained on a Lambda-900 UV/vis/NIR spectrophotometer (Perkin Elmer). The current-voltage (I-V) curves were measured with a Keithley 238 source measurement unit. All thin films preparation and measurements were carried out at room temperature in air.
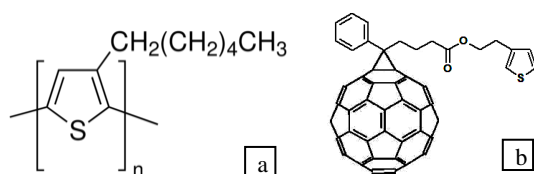
* bushra_omer4@yahoo.com

Fig. 1 – Chemical structure of (a) poly (3-Hexylthiophene) and (b) [6, 6]-Phenyl C61-Butyric Acid 3-Ethylthiophene Ester
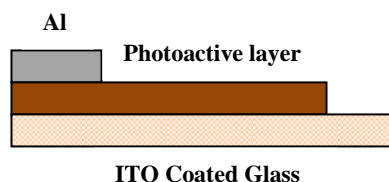

Fig. 2 – Schematic of the polymer solar cell device structure

3. RESULTS AND DISCUSSIONS

Fig. 3 shows the absorption of thin films made from pure poly (3-Hexylthiophene), pure [6, 6]-Phenyl C61-Butyric Acid 3-Ethylthiophene Ester and (3:1) poly (3-Hexylthiophene): [6, 6]-Phenyl C61-Butyric Acid 3-Ethylthiophene Ester composite at room temperature. All the thin films were spin coated from 1,2 dichlorobenzene. The absorption maximum (λ_{max}) of P3HT can be observed at 556 nm (2.23 eV) and two shoulders appeared at 532 nm and 605 nm. The optical band gap of P3HT is determined with a tangential through the turning point of the low energy side of the spectra, leading to estimated value of 1.89 eV. The absorption maximum of P3HT in the composite films was found to be around 574 nm (18 nm red shifted compared to pure P3HT), the shoulders appeared at 542 nm and 623 nm. From the absorption spectra of the composites it was very clear that the two peaks at (281 nm and 354 nm) are belong to the modified fullerene. It was noticeable that the absorption spectra of the composites are just superpositions of the absorption spectra of the individual components.
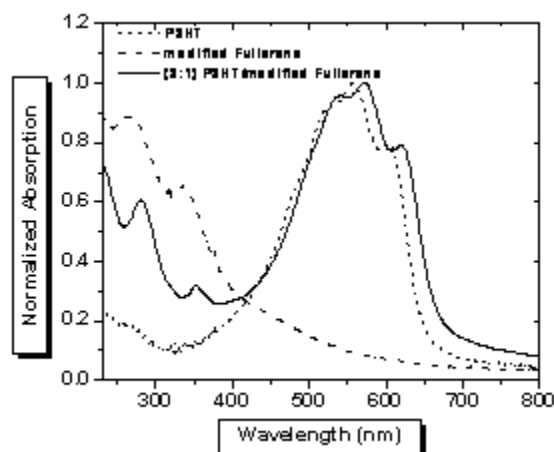

Fig. 3 – Absorption spectra of pure P3HT, pure modified Fullerene and P3HT: modified Fullerene (3:1) composite films

Fig. 4 shows the current density-voltage characteristics of the device in dark; we observe that the forward current is exponentially increased with applied voltage; this is an indication of the diode characteristics. The device shows a high rectification ratio (γ) of about 392 at ($\pm$ 1.5 V), the diode is regarded as well rectified.
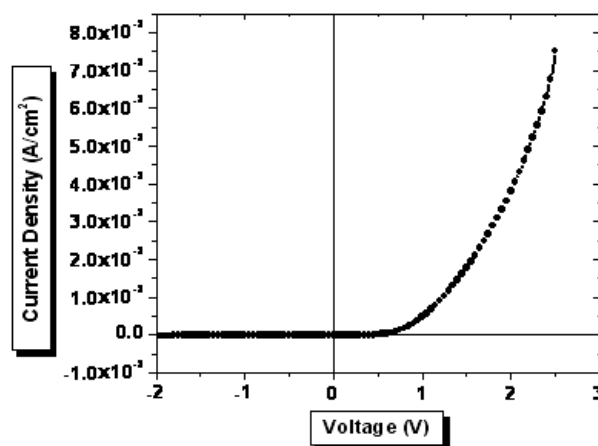

Fig. 4 – Current density-voltage characteristics under dark for (3:1) P3HT / modified fullerene device structure

Fig. 5 shows a semi-logarithmic plot of the current density versus the applied voltage of the device, in dark at room temperature. The general diode equation,

$$J = J_0 \left[\exp \left(qV / nKT \right)^{-1} \right], \tag{1}$$

describes the J-V characteristics of both *p-n* junctions and Schottky diodes. Here, *V* is the applied voltage, *n* is the ideality factor, *q* is the electron charge, *K* is the Boltzmann constant, *T* is the temperature and J_0 is the saturation current derived from the straight line intercept of ln *J* at *V* = 0 and is given by:

$$J_0 = A^* T^2 \exp \left(- q \varphi_b / KT \right), \tag{2}$$

where $A^* = 120$ A/cm^2 K^2 is the effective Richardson constant for an electron in free space and φ_b the zero-bias potential barrier height. The ideality factor n is unity in the Shockly theory for *p-n* junctions in the absence of recombination, as well as for thermionic emission theory and diffusion theory for Schottky diodes. The slope of the logarithmic plot is related to the ideality factor n through:

$$1 / n = (KT / q) (d (\ln J) / dV), \tag{3}$$

Once J_0 is found, we can find the barrier height per unit charge using the relation:

$$\Phi_b = (KT / q) \ln(A^* T^2 / J_0), \tag{4}$$

From ln *J* versus *V* characteristics in the dark, shown in Fig. 5 and making use of equations (1), (2), (3) and (4) the value of the saturation current determined as 3.16×10^{-9} A/cm^2. The ideality factor *n* and the barrier hight φ_b was found to be 2.45 and 0.78 eV, respectively. The deviation of the ideality factor of the dark current from unity may be due to a trap-assisted recombination.

At high bias the outflow rate of the injected carriers is reduced greatly and charges accumulate in the bulk of the semiconducting organic layer and that is due to low charge carrier mobility as well as the presence of
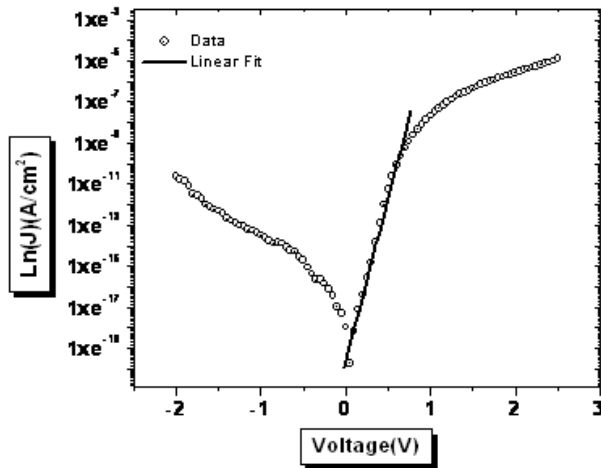
Fig. 5 – Semi-logarithmic plot of Current density-Voltage characteristics in the dark

Fig. 6 – Current density-Voltage characteristics at high bias in dark

traps. In this case the transport flow is dominantly controlled by the space charge limited current (SCLC) resulting into saturation of current. The relation between the current density and voltage in free-traps SCLC is given by the Childs law [12]:

$$J = (9/8)(\varepsilon\mu / d^3)V^2 \qquad (5)$$

where μ is the charge carrier mobility and d is the film thickness.

In presence of traps with exponential trap distribution the SCLC takes a power law dependence of the form:

$$J = K V^{m+1} \qquad (6)$$

where m is defined in terms of a characteristics trap distribution constant.

Plot of the current density versus voltage at high forward bias, beyond 1 V is shown in Fig. 6. The current density depends super linearly on the forward voltage. From the fit we could find the relation:

$$J = 5.5 \times 10^{-4} V^{2.8} \qquad (7)$$

The correlation coefficient was good ($R = 0.998$). Comparing equation (7) with (6) we get $K = 5.5 \times 10^{-4}$ and $m = 1.8$, this is indicative of electrical transport that is dominated by SCLC with exponential trap distribution. The overall parameters for the J-V curve under dark were tabulated in Table 1.

Table 1 – The photovoltaic parameters under dark

Parameters	J_0(A/cm^2)	Φ_b (eV)	γ	n
Value	3.16×10^{-9}	0.78	392	2.45

Fig. 7 shows the current density versus the voltage curves in dark and when the device was illuminated through the ITO (front) side with an incident light intensity of about 2.8 mW/cm^2 from a projector lamb. The current in the reverse direction is strongly increased by the illumination. This indicates that the light illumination increases the production of electron-hole pairs. At higher forward bias, the dark and photocurrent are quite similar, indicating that photoconductivity does
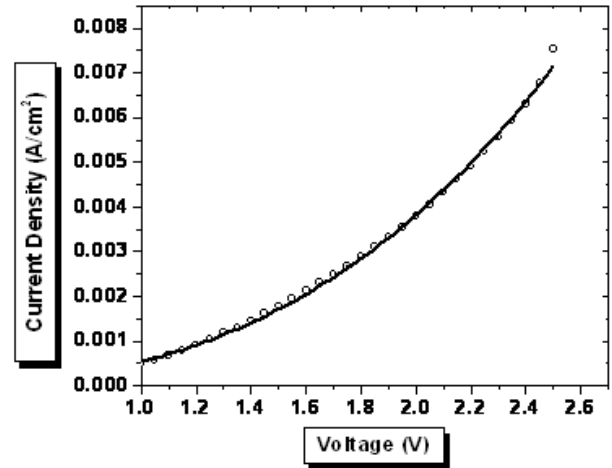
not play an important role in the device. The device shows photovoltaic behavior with an open circuit voltage of 400 mV, short circuit current of 22.9 μA/cm^2, fill factor of 0.32, and a power conversion efficiency of 0.105 %. The short circuit current of our device is small because the work function of the ITO has a boor matching with the highest occupied molecular orbital level of the P3HT. This in turn expected to decrease the whole transport and collection at the anode. According to the metal-insulator-metal (MIM) model for non-ohmic contacts devices, the open circuit voltage is determined by the work function difference of the materials used for the electrodes, Al (4.3 eV) [6, 12] and ITO (4.7 eV) [6, 12] results V_{oc} in the range of 0.4 V, which agree very well with the experimentally observed open circuit voltage.
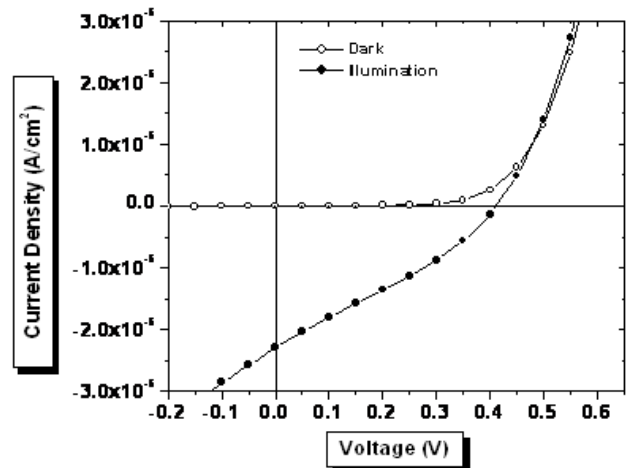

Fig. 7 – Current density-voltage characteristics of P3HT / modified fullerene blend, 3:1 ratio

4. CONCLUSIONS

In summary, we have fabricated Poly (3-Hexylthiophene): [6, 6]-Phenyl C61-Butyric Acid 3-Ethylthiophene photovoltaic cell. The dark current density-voltage characteristics indicates a non-ideal diode behavior with ideality factor n (2.45), barrier

height φ_b (0.78 eV) and a rectification ratio of about 392 at ± 1.5 V. Under illumination the device gave an open circuit voltage of 400 mV, short circuit current of 22.9 μA/cm² and fill factor of 0.32.

REFERENCES

1. N.S. Sariciftci, D. Braun, C. Zhang, V.I. Srdanov, A.J. Heeger, G. Stucky, F. Wudl, *Appl. Phys. Lett.* **62**, 585 (1993).
2. Abay Gadisa, Bantikassegn Workalemahu, *Synthetic Met.* **129**, 179 (2002).
3. L.S. Roman, M. Berggren, O. Inganas, *Appl. Phys. Lett.* **75**, 3557 (1999).
4. Lionel Sicot, Bernard Geffroy, Andre Lonin, Paul Raimond, Carole Sentein, Jean Michel Nunzi, *J. Appl. Phys.* **90**, 1047 (2001).
5. G. Dennler, C. Lungenschmied, H. Neugebauer, N.S. Sariciftci, A. Labouret, *J. Mater. Res.* **20**, 3224 (2005).
6. Maher Al-Ibrahim, H. Klaus Roth, Uladzimir Zhokhavets, Gerhard Gobsch, Steffi Sensfuss, *Sol. Energ. Mat. Sol. C.* **85**, 13 (2005).
7. Zhicai He, Chengmei Zhong, Shijian Su, Miao Xu, Hongbin Wu, Yong Cao, *Nature Photonics* **6**, 591 (2012).
8. G. Yu, J. Gao, J.C. Hummelen, F. Wudl, A.J. Heeger, *Science* **270**, 1789 (1995).
9. Daisuke Sukeguchi, Surya Prakash Singh, Mamidi Ramesh Reddy, Hideyuki Yoshiyama, Rakesh A. Afre, Yasuhiko Hayashi, Hiroki Inukai, Tetsuo Soga, Shuichi Nakamura, Norio Shibata, Takeshi Toru, *Beilstein J. Org. Chem.* **5**, No. 7 (2009).
10. C.J. Brabec, A. Cravino, D. Meissner, N.S. Sariciftci, M.T. Rispens, L. Sanchez, J.C. Hummelen, T. Fromherz, *Thin Solid Films* **403-404**, 368 (2002).
11. Floris B. Kooistra, Joop Knol, Fredrik Kastenberg, Lacramioara M. Popescu, Wiljan J.H. Verhees, Jan M. Kroon, Jan C. Hummelen, *Org. Lett.* **9**, 551 (2007).
12. D. Chirvase, Z. Chiguvare, M. Knipper, J. Parisi, V. Dyakonov, J.C. Hummelen, *Synthetic Met.* **138**, 299 (2003).